

High Resolution Spectroscopy and Spectropolarimetry of some late F-/early G-type sun-like stars as targets for Zeeman Doppler imaging.

I.A. Waite^{A,D}, S.C. Marsden^{B,A}, B.D. Carter^A, E. Alécian^C, C. Brown^A, D. Burton^A, and R. Hart^A

^A Faculty of Sciences, University of Southern Queensland, Toowoomba, 4350, Australia

^B Centre for Astronomy, School of Engineering and Physical Sciences, James Cook University, Townsville, 4811, Australia

^C LESIA, Observatoire de Paris-Meudon, F-92195 Meudon Cedex, France

^D Email: contact.waite@usq.edu.au

Abstract: High resolution spectroscopy and spectropolarimetry have been undertaken at the Anglo-Australian Telescope in order to identify suitable targets for magnetic studies of young sun-like stars, for the proxy study of early solar evolution. This study involved the investigation of some variable late F-/early G-type sun-like stars originally identified by the Hipparcos mission. Of the 38 stars observed for this study, HIP 31021, HIP 64732, HIP 73780 were found to be spectroscopic binary stars while HIP 19072, HIP 67651 and HIP 75636 are also likely to be binaries while HIP 33111 could even be a triple system. Magnetic fields were detected on a number of the survey stars: HIP 21632, HIP 43720, HIP 48770, HIP 62517, HIP 71933, HIP 77144, HIP 89829, HIP 90899 and HIP 105388, making these stars good candidates for follow-up Zeeman Doppler imaging studies.

Keywords: stars: activity — stars: chromospheres — stars: magnetic fields — stars: spots and rotation

1 Introduction

The study of young sun-like stars provides a window onto the Sun's intensely active past and an understanding of early solar evolution. In particular, the observations of starspots and associated magnetic activity gives clues to the underlying dynamo processes operating in young sun-like stars. Thus, the study of magnetic fields helps us understand the solar interior as well as its atmosphere. A key question in this respect is: how does the young Sun differ in its internal structure and energy transport systems when compared with the modern-day Sun? The technique of Zeeman Doppler imaging (ZDI) (Semel 1989; Semel et al. 1993; Donati et al. 2003) can be used to map the magnetic topologies of rapidly rotating young sun-like stars to help address this question.

In the Sun today, strong shear forces are formed at the interface between the solid-body rotation of the radiative zone and the differentially rotating convective layer in a region called the tachocline. In the tachocline differential rotation wraps north-south magnetic field lines around the Sun in the direction of rotation and convective motions act to raise the magnetic fields through the convection zone to emerge at the surface. This interaction converts the global poloidal magnetic field to a toroidal field. This effect is known as the “ Ω -effect”. The α -effect is the reverse process, converting the global toroidal field to the poloidal field. In contrast, studies by Donati et al. (2003) of K-dwarf stars and by Marsden et al. (2011a,b) and Waite et al. (2011) of pre-main-sequence G-type stars show regions

of azimuthal fields. Donati et al. (2003) interpret this in terms of an $\alpha^2\Omega$ dynamo process (Brandenburg et al. 1989; Moss et al. 1995) being distributed throughout the entire convection zone and close to the surface of the star itself.

The Sun today undergoes activity cycles in the form of magnetic reversals, but at what stage do these cycles begin during the early evolution of the star? Recent theoretical work by Brown et al. (2010) has suggested that young stars undergo “attempted” field reversals, where the magnetic field begins to break-up, a signature of an impending reversal, only to reinforce again in the original direction. Resolving the origin of the solar dynamo will help us address the more general question of how stellar magnetic cycles develop in young stars, and affect any attendant emerging planetary systems. The search for ZDI targets is thus motivated by the need to study a sample of young Suns to test recent dynamo theory for these stars.

The initial search for potential ZDI targets by Waite et al. (2005) found two pre-main-sequence stars: HD 106506 and HD 141943. ZDI has been used to map the magnetic topologies of HD 106506 (Waite et al. 2011) and evolution of the magnetic topologies and variations in the surface differential rotation of HD 141943 (Marsden et al. 2011a,b). This paper is a follow-on from this initial search for late F-/ early G-type stars. Our search specifically aims to measure the projected rotational velocity, $v\sin i$, radial velocity, the level of magnetic and chromospheric activity, and confirm the expected youthful evolutionary status of these stars for studying the origins of the magnetic dynamo in young sun-like

stars.

2 Observations at the Anglo-Australian Telescope

2.1 Selection criteria

The Hipparcos space mission (Perryman et al. 1997) has provided a wealth of stellar astrometry, and revealed many previously unknown variable stars. A large number of these unresolved variables (Koen & Eyer 2002) are likely to be eclipsing binaries, but some are expected to be active stars with starspot modulation. From the Hipparcos database, late F-/early G-type unresolved variable stars were extracted from the original list of Koen & Eyer (2002). To reduce the sample to a manageable number of stars, only those sun-like stars with a variability between ~ 0.04 and ~ 0.1 magnitude were selected. If the variability was less than 0.04, the spot activity (if the variability was due to starspots) on the star would unlikely be sufficient to deform the stellar profiles sufficiently for any spatial information to be recovered using the technique of Doppler imaging (DI). Any variation above ~ 0.1 would most likely be a result of a companion star. A final list of 38 stars was compiled for follow-up high-resolution spectroscopy and spectropolarimetry at the Anglo-Australian Telescope (AAT).

2.2 Spectroscopy

High-resolution spectra of 38 late F-/early G-type stars were observed over two nights of Service observations on the 14th of April and 7th of September, 2008 using the University College of London Échelle Spectrograph (UCLES) at the AAT. The EEV2 chip was used with the central wavelength set to 526.8 nm. The 31 lines per mm grating was used with a slit width of 0.73 mm and slit length of 3.18 mm for observations on the 14th April while the slit width was set to 0.74 mm and slit length of 3.17 mm was set for observations on the 7th September, 2008. This gave an approximate resolution of 50500, extending from order #84 to order #129. A journal of the observations is shown in Table 1.

2.3 Spectropolarimetry

Follow-up spectropolarimetric observations of stars that exhibited rapid rotation were undertaken on a number of Director's nights at the AAT using the Semel Polarimeter (SEMPOL) (Semel 1989; Semel et al. 1993; Donati et al. 2003). Again the EEV2 chip was used, with a central wavelength of 526.8 nm and coverage from 437.6497 nm to 681.8754 nm. The dispersion of ~ 0.002481 nm at order # 129, with an average resolution across the chip of approximately $\sim 70\,000$. Observations in circular polarisation (Stokes V) consists of a sequence of four exposures. After each of the exposures, the half-wave Fresnel Rhomb of the SEMPOL polarimeter was rotated between $+45^\circ$ and

-45° so as to remove instrumental polarisation signals from the telescope and the polarimeter. Section 3.5 gives more details regarding spectropolarimetric observations while more details on the operation of SEMPOL is given in Semel et al. (1993), Donati et al. (1997) and Donati et al. (2003). A journal of the observations is shown in Table 2.

2.4 Data Analysis

The aim of this project is to determine the projected rotation velocity ($v \sin i$), radial velocity, level of magnetic and chromospheric activity and estimate the age of each of the targets. The chromospheric activity indicators included the $H\alpha$, magnesium triplet and sodium doublet spectral lines. The LiI 670.78 nm spectral line was used as an age indicator. The initial data reduction was completed using the ESPRIT software package (Échelle Spectra Reduction: An Interactive Tool, (Donati et al. 1997)). The technique of Least Squares Deconvolution (LSD) (Donati et al. 1997) was applied to each spectra. LSD assumes that each spectral line in the spectrum from a star can be approximated by the same line shape. LSD combines several thousand weak absorption lines to create a high signal-to-noise (S/N) single-line profile. Whereas the average S/N of a typical profile was ~ 50 -100, the resulting LSD profile has a combined S/N of the order of 1000 or higher. This substantial multiplex gain has the advantage of removing the noise inherent in each line profile while preserving Stokes I and V signatures. The line masks that were used to produce the LSD profile were created from the Kurucz atomic database and ATLAS9 atmospheric models (Kurucz 1993) and were closely matched to the spectral type of each individual star.

3 Results and Analysis

3.1 Projected Rotational Velocity

The projected rotational velocity, $v \sin i$, was measured by rotationally broadening a solar LSD profile to match the LSD profile of the star. This method was shown to be reliable, particularly with rapidly rotating stars, by Waite et al. (2005) when they compared this technique with the Fast Fourier Transform technique of Gray (1992). Table 1 shows the projected rotational velocities for the target stars. The error bars on each measurement are usually $\pm 1 \text{ km s}^{-1}$, however, for rapidly rotating stars with substantial deformation of the line profiles due to spot features, the errors could increase to $\pm 3 \text{ km s}^{-1}$ or higher. Many of these $v \sin i$ values have not been previously determined.

The term Ultrafast Rotator (UFR) has been used extensively in the literature but without an explicit definition being applied. Hence the need to refine this terminology, particularly for solar-type stars. Stars that have projected rotational velocities less than 5 km s^{-1} will be considered as Slow Rotators (SR) as this is the lower limit at which we can accurately measure the $v \sin i$ of the star in this dataset. Those stars with $v \sin i$ between 5 km s^{-1} and 20 km s^{-1} will be con-

Table 1: Journal of observations using UCLES at the AAT.

HIP	Spectral Type	UTSTART	Exp Time (sec)	S/N ^a	v_{rad}^b km s ⁻¹	$v \sin i^b$ km s ⁻¹	EEW ^c H α (mÅ)	EqW ^d Li (mÅ)
UTDATE	2008, APR 14							
23316	G5V ¹	10:13:49	600	77	22.8	~ 6	330 \pm 6	198 \pm 7
27518	G3 ²	10:26:08	400	72	5.2	<5	-46 \pm 19	<5
31021 ^e	G3V ³	10:48:24	400	73	—	—	—	—
33111 ^f	G5V ¹	10:57:02	400	79	—	—	—	—
33699	F8V ⁴	11:05:36	400	59	29.8	<5	56 \pm 10	41 \pm 3
41688	G6IV/V ⁶	11:15:18	60	46	-20.4	<5	62 \pm 10	66 \pm 10
43720	G1V ¹	11:18:17	400	62	2.2	38	400 \pm 28	<5
46949	G2/3V ⁵	11:26:48	600	64	26.8	<5	23 \pm 11	68 \pm 3
48146	G6IV/V ⁶	11:39:30	600	49	0.5	<5	43 \pm 9	68 \pm 1
48770	G7V ¹	11:52:21	1200	67	19.6	35	990 \pm 90	234 \pm 5
60894	G0/1V ⁷	12:14:57	600	29	29.4	<5	-36 \pm 30	<5
62517	G0 ⁸	12:27:56	400	68	-25.5	52	265 \pm 25	47 \pm 24
63734	F7/8V ⁹	12:36:18	200	97	1.3	~ 6	121 \pm 11	141 \pm 6
63936	F8 ⁸	12:42:02	600	70	-10.0	<5	80 \pm 8	<5
64732 ^e	F5V ⁶	12:54:22	150	84	—	—	—	—
66387	G0 ⁸	12:59:05	600	55	-24.1	<5	48 \pm 6	<5
67651 ^g	F8 ¹⁰	13:10:25	400	57	—	—	—	—
68328	G0 ¹¹	13:20:13	600	76	8.8	~ 6	850 \pm 45	263 \pm 4
69338	G1V ⁶	13:32:39	300	81	-8.6	<5	9 \pm 2	61 \pm 3
70053	G0 ⁸	13:39:00	450	68	7.8	<5	17 \pm 7	45 \pm 4
71933	F8V ¹	13:57:17	150	84	6.0	75	274 \pm 25	139 \pm 7
		15:20:59	150	82	-1.9	75	"	"
71966	F7V ³	14:01:16	450	75	9.3	<5	90 \pm 10	30 \pm 3
73780 ^e	G0IV/V ⁷	14:10:35	300	77	—	—	—	—
75636 ^g	G9V ¹	14:17:19	900	88	43.7	50	820 \pm 90	<5
77144	G1V ¹¹	14:33:28	450	93	-1.6	65	466 \pm 24	207 \pm 7
79090	F8 ⁸	14:43:39	600	60	6.1	<5	56 \pm 12	46 \pm 4
79688	G1V ⁵	14:56:07	200	86	12.6	11	172 \pm 12	13 \pm 5
89829	G5V ¹	15:01:17	200	74	-10.6	114	280 \pm 52	211 \pm 13
		15:25:42	200	75	1.2	114	"	"
90899	G1V ¹²	15:06:00	450	82	-2.7	19	408 \pm 14	176 \pm 6
93378	G5V ¹	15:16:07	150	76	—	225	0	322 \pm 56
		15:30:48	150	68	—	229	"	"
		16:11:01	200	62	—	226	"	"
105388	G7V ¹	16:04:01	300	58	-1.8	17	520 \pm 50	216 \pm 5
UTDATE	2008, SEPT 7							
5617	G2/3 ⁷	13:49:05	400	70	56.5	<5	—	<5
10699	G7IV ¹	13:58:52	600	82	39.1	7	220 \pm 20	32 \pm 3
11241	F8V ⁹	14:13:43	400	83	-3.5	<5	164 \pm 8	98 \pm 3
19072 ^f	F8 ⁸	18:19:56	240	79	—	—	—	—
		18:56:21	240	71	—	—	—	—
20994	G0 ⁸	18:25:13	900	74	57.8	<5	85 \pm 31	44 \pm 2
21632 ^h	G3V ¹	14:23:12	400	81	19.5	18	385 \pm 21	190 \pm 2
		19:04:37	400	97	19.3	18	517 \pm 32	"
25848	G0 ¹³	18:42:35	600	68	27.3	69	668 \pm 60	250 \pm 13
		19:13:43	600	65	28.7	69	"	"

^aS/N: Mean Signal-to-noise at Order 107, which was the centre of the spectrum. ^bThe radial velocity (v_{rad}) and projected rotational velocity ($v \sin i$). The errors are estimated to be ± 1 km s⁻¹, although for rapidly rotating stars with substantial deformation of the line profiles due to spot features, the errors could increase to ± 3 km s⁻¹ or higher. ^cEEW H α : Emission equivalent width of the H α line, see Section 3.3. ^dEqW Li: Equivalent width for the Li-670.78 nm spectral line. ^eBinary system. ^fPossible triple system. ^gPossible binary system. ^hThis star has shown variation in the H α profile hence both measurements for the emission equivalent width have been given.

¹Torres et al. (2006), ²Jackson & Stoy (1954), ³Houk & Cowley (1975), ⁴Rousseau, Perie & Gachard (1996), ⁵Houk (1982), ⁶Houk & Swift (1999), ⁷Houk (1978), ⁸SAO Catalogue (1966), ⁹Houk & Smith-Moore (1988), ¹⁰Dieckvoss & Heckmann (1975), ¹¹Sartori, Lépine, & Dias (2003), ¹²Turon et al. (1993), ¹³Li & Hu (1998)

Table 3: Classification of Solar-type stars based on projected rotational velocities.

Classification	$v \sin i$ range (km s^{-1})
Slow Rotator (SR)	0 - < 5
Moderate Rotator (MR)	5 - < 20
Rapid Rotator (RR)	20 - < 100
Ultra-Rapid Rotator (URR)	100 - < 200
Hyper-Rapid Rotator (HRR)	200+

sidered as Moderate Rotators (MR). This upper limit is considered a critical velocity where dynamo saturation has been theorised to slow the angular momentum loss of rapidly rotating stars (e.g. Irwin (2007); Krishnamurthi (1997); Barnes & Sofia (1996)). Below 20 km s^{-1} , the strength of the star’s magnetic dynamo is related to the star’s rotation rate but above this speed, it is believed that dynamo saturation is occurring where the strength of the star’s magnetic dynamo is no longer dependent upon stellar rotation. One empirical measure of this saturation in young solar-type stars is coronal X-ray emission. This emission, defined as the ratio of the star’s X-ray luminosity to that of the star’s bolometric luminosity (Vilhu 1984), increases as rotation increases when it plateaus at the $v \sin i$ of 20 km s^{-1} . Stauffer et al. (1997) theorised that this is consistent with dynamo saturation. Those stars with $v \sin i$ greater than 20 km s^{-1} to 100 km s^{-1} will be referred to as Rapid Rotators (RR). The upper limit of $\sim 100 \text{ km s}^{-1}$ was selected as at this rotational speed, the X-ray luminosity decreases below the saturated level (Randich 1998), an effect that Prosser et al. (1996) called supersaturation. These definitions are consistent with those used by Marsden, Carter, & Donati (2009), Marino et al. (2003) and Prosser et al. (1996). Those stars between 100 km s^{-1} to 200 km s^{-1} will be referred to as Ultra-Rapid Rotators (URR). Stars that exceed 200 km s^{-1} will be referred to as Hyper-Rapid Rotators (HRR) and are likely to be very oblate. However many of the stars in this sample have not had their inclination determined, thus the $v \sin i$ is likely to be an underestimate of the true equatorial rotation of the star, and thus depending on the inclination, the star may be more rapidly rotating than indicated by the $v \sin i$. In addition, we limit these definitions to solar-type stars. Table 3 gives a summary of the definitions used in this paper.

3.2 Heliocentric Radial Velocity

Each spectrum, when extracted, was shifted to account for two effects. Initially, small instrumental shifts in the spectrograph were corrected for by using the positions of the telluric lines embedded in each spectrum. A telluric line mask was used to produce an LSD profile and the exact position of this profile was used to determine these small corrections (Donati et al. 2003). Secondly, the heliocentric velocity of the Earth towards the star was determined and corrected for.

The LSD profile of the star was used to measure the radial velocity of the star by first re-normalising the profile, then fitting a gaussian curve to the profile and measuring the location of the minimum. The radial velocities are listed in Table 1. The error in the radial velocity was estimated to be $\pm 1 \text{ km s}^{-1}$ although the presence of spots on the surface did have some effect on the location of the minimum, especially on stars with rotational speeds in excess of 100 km s^{-1} such as HIP 89829 where the fitting of the gaussian profile was problematic given the rapid rotation. The large variation seen in the radial velocity measurements for HIP 89829 could be a result of this star being a binary star. However, we have searched for evidence of a companion star deforming the LSD profile of the spectropolarimetry data and conclude that this star is probably single. This still does not preclude the existence of a secondary component as a very low mass companion such as an M-dwarf is likely to modify the radial velocity of the primary without generating a detectable line in the LSD profile, because the line-mask employed here is optimised for the primary, not for the companion. It was impossible to accurately measure the radial velocity of the HRR HIP 93378 due to its extreme deformation of the LSD profiles.

3.3 Chromospheric Indicators: Hydrogen α , Magnesium-I triplet and Sodium-I doublet.

The $\text{H}\alpha$, magnesium-I triplet (516.733, 517.270 and 518.362 nm) and sodium D_1 and D_2 doublet (588.995 and 589.592 nm) lines are often used as proxies for stellar activity and in particular chromospheric activity. The $\text{H}\alpha$ line is formed in the middle of the chromosphere (Montes et al. 2004) and is often associated with plages and prominences. The magnesium I triplet and sodium D_1 and D_2 doublet lines are collisionally dominated and are formed in the lower chromosphere and upper photosphere. This makes them good indicators of changes in that part of the atmosphere of stars (Montes et al. 2004). Many authors (e.g. Zarro & Rodgers (1983), Young et al. (1989), Soderblom et al. (1993a), Montes et al. (2004), Waite et al. (2005)) determine the emission component of the $\text{H}\alpha$ line by subtracting the stellar spectrum from a radial velocity-corrected, inactive star that has been rotationally broadened to match the $v \sin i$ of the target. This technique is temperature dependent, but since all of our targets have similar spectral types, a solar spectrum was used as the inactive standard star in this survey. The resulting emission equivalent width (EEW) is a measure of the active chromospheric component of these spectral lines, including the $\text{H}\alpha$ line. Figure 1 shows the core emission of the magnesium triplet and $\text{H}\alpha$ line for the more active stars in this sample. Many of the likely targets for ZDI exhibit core emissions; however, the HRR star HIP 93378 exhibits no activity in either the magnesium triplet or the $\text{H}\alpha$ line. This may be due to the extreme broadening of the spectral lines “washing out” the emission component.

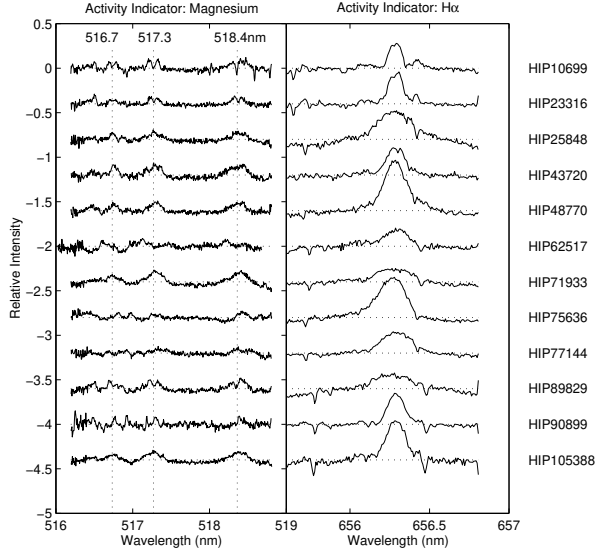


Figure 1: The core emission in the magnesium triplet lines, left panel, and the H α spectral line, right panel, are shown for rapid rotators in this sample. This core emission was obtained by subtracting a radial velocity corrected, rotationally-broadened solar spectrum.

3.4 Lithium-I 670.78-nm: An Age Indicator

In the absence of a companion star, an enhanced Li I 670.78 nm line can be used as an indicator of youth (Martín & Claret 1996) for stars that are cooler than mid-G type ($0.6 \leq B-V \leq 1.3$) although this is not as useful for F-type stars where there appears to be a plateau in the depletion of the lithium due to age (Guillout et al 2009). However, do Nascimento, da Costa, & de Medeiros (2010) point out that there is a large range in lithium depletion for solar-type stars which may reflect different rotational histories or as a result of different mixing mechanisms such as shear mixing caused by differential rotation (Bouvier 2008). In analysing the spectra, the equivalent width EW_{Li} was measured using the SPLOT task in IRAF. This was done so as to allow comparison with those measured by Torres et al. (2006). The error in the measured values of EW_{Li} is primarily due to uncertainties in the continuum location. When the rotational velocity, $v \sin i$, exceeded 8 km s^{-1} , the Li I spectral line is blended with the nearby 670.744 nm Fe I line. This was corrected using the same correction factor developed by Soderblom et al. (1993a,b). The correction used is shown in equation 1.

$$EW_{Li,corr} = EW_{Li} - 20(B - V) - 3 \quad (1)$$

Some of the results appear slightly discrepant when compared with Torres et al. (2006). It is unclear whether Torres et al. (2006) corrected for the Fe I line in their measurements but such a difference in processing may possibly explain the discrepancies. Figure 2 shows the

strength of the Li I 670.78 nm line, compared with the nearby Ca I 671.80 nm line, for a number of stars that are likely to be future targets for the ZDI programme.

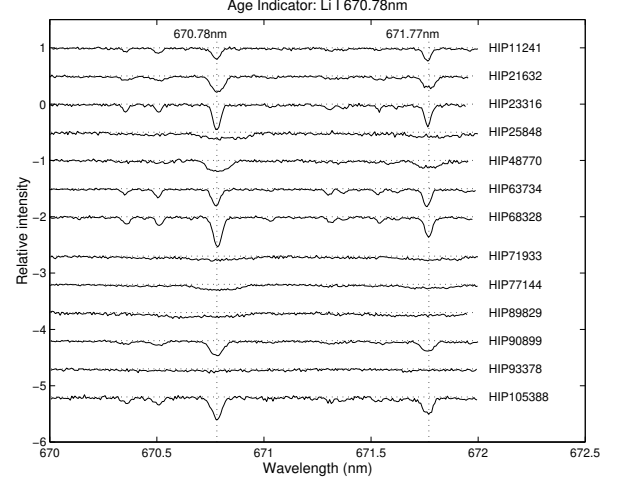


Figure 2: The lithium-I 670.78 nm line, compared with the calcium-I 671.77 nm line, for a number of stars in this survey.

3.5 Spectropolarimetry

The magnetic signatures embedded in starlight are extremely difficult to detect. The typical Zeeman signature is very small, with a circular polarisation signature (Stokes V) of $\sim 0.1\%$ of the continuum level for active stars (Donati et al. 1997). As discussed in Section 2.3, observations in Stokes V consists of a sequence of four sub-exposures with the half-wave Fresnel Rhomb being rotated between $+45^\circ$ and -45° . To detect these signatures, LSD is applied to increase the signal-to-noise of the signature when creating the Stokes V profile. The Stokes V profile is the result of constructively adding the individual spectra from the four exposures by “pair-processing” sub-exposures corresponding to the opposite orientations of the half-wave Fresnel Rhomb. To determine the reliability of the process, a “null” profile is produced as a measure of the noise within the LSD process. This null profile is found by “pair-processing” sub-exposures corresponding to the identical positions of the half-wave Fresnel Rhomb of the SEMPOL polarimeter during each sequence of 4 sub-exposures.

When producing figures, such as Figure 3 for example, the Stokes V (upper) and null (middle) profiles have been multiplied by 25 so as to show the variation within each profile. Both profiles have been shifted vertically for clarity. The dots on the Stokes V and null profiles are the actual data while the smooth curve is a 3-point moving average. The deformation in the Stokes V profile is a direct result of the magnetic field observed on the star while deformation in the Stokes I (intensity) profile (lower) is a result of starspots on the surface of the star. For more information on ZDI

see Carter et al. (1996) and Donati et al. (1997).

For each observation a false-alarm probability (FAP) of magnetic field detection was determined. FAP is a measure of the chance of the signal found in the Stokes V profile being a result of noise fluctuations rather than a real magnetic detection. The FAP is based on a χ^2 probability function (Donati, Semel, & Rees 1992) and is estimated by considering the reduced χ^2 statistics both inside and outside the spectral lines, as defined by the position of the unpolarised LSD profiles, for both the Stokes V and the null profiles (Donati et al. 1997). The FAP for each observation is listed in Table 2. A definite magnetic detection in the Stokes V was considered if the associated FAP was smaller than 10^{-5} (i.e. χ^2 probability was larger than 99.999 %) while a marginal detection was observed if the FAP was less than 10^{-3} but greater than 10^{-5} . In addition to this, the signal must only have been detected in the Stokes V profile and not within the null profile, and be within the line profile velocity interval, from $v_{rad} - v \sin i$ to $v_{rad} + v \sin i$. This criteria is consistent with the limits used by Donati et al. (1997).

4 Some comments on individual stars

Many of the stars in this survey exhibited some indication of activity either due to the presence of a companion star, or in the case of single stars, activity due to youth and/or rapid rotation. We will consider each likely ZDI target in more detail in this section.

4.1 Moderate and rapid rotators suitable for ZDI studies

4.1.1 HIP 21632

HIP 21632 is a G3V star (Torres et al. 2006). The Hipparcos space mission measured a parallax of 18.27 ± 1.02 milli-arcseconds (mas) (van Leeuwen 2007), giving a distance of 178_{-9}^{+11} light-years (ly). Using the bolometric corrections of Bessell, Castelli, & Plez (1998) and the formulations within that paper, the effective temperature of this star was determined to be 5825 ± 45 K and the radius was estimated to be $0.96 \pm 0.04 R_{\odot}$. The luminosity was subsequently estimated to be $0.93_{-0.11}^{+0.12} L_{\odot}$. Zuckerman & Song (2004) proposed that HIP 21632 was a member of the Tucana/Horologium Association indicating an age of ~ 30 Myr. This star has an emission equivalent width for the $H\alpha$ line in the range from ~ 385 mÅ to ~ 517 mÅ demonstrating the presence of a very active, and variable, chromosphere. This variation could be due to prominences occurring on this star. Two exposures, separated by 4 hours 41.41 minutes, were taken on April 14, 2008 demonstrated noticeable variation in the core emission of the $H\alpha$ line, as shown in Figure 4. Yet there was no variation in the magnesium triplet and indeed, there was very little core emission in the three lines, with some filling-in in the wings of the lines. However, there were some minor changes in the sodium D_1 line but the variation is no

where near as pronounced as in the mid-level chromospheric level. There is no evidence of the presence of a companion star in the LSD profile. Torres et al. (2006) measured a radial velocity of 18.8 km s^{-1} (using cross correlation methods) and an equivalent width for the LiI line of 200 mÅ. These values are consistent with the values obtained from this survey of an average radial velocity of $19.4 \pm 1 \text{ km s}^{-1}$ and a equivalent width for the LiI line of $190 \pm 2 \text{ nm}$ (see Section 3.4 on a possible reason for slightly discrepant values).

This star was observed spectropolarimetrically on two occasions using SEMPOL. On the first occasion, a no magnetic signal was detected with a mean S/N of 5898 with 4 sub-exposures, yet achieved a definite magnetic detection with only 2 sub-exposures with a mean S/N of 2710 on the second occasion. The resulting LSD profile for this cycle is shown in Figure 3. Whereas this star is only a moderate rotator, it is a worthwhile target for more detailed spectropolarimetric studies.

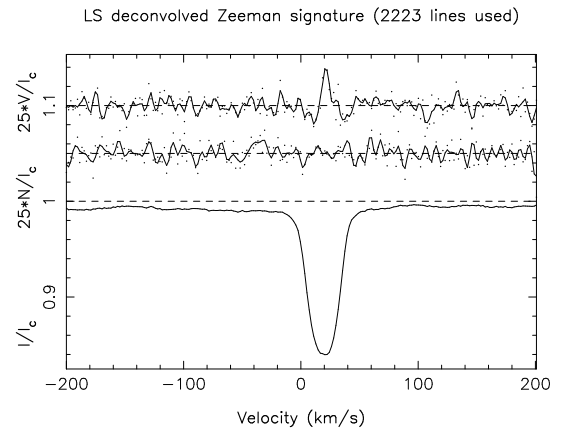


Figure 3: The magnetic detection of young G3V star HIP 21632. The lower profile is the Stokes I LSD profile, the middle profile is the null profile and the upper profile is the Stokes V profile. The dots are the actual data while the smooth line is a moving 3-point average of the data. The Stokes V and Null profiles have been vertically shifted for clarity. In addition to this, the Stokes V and Null profiles each were multiplied by 25 in order to highlight the actual signatures. The Stokes V profile clearly shows a strong magnetic detection. This was achieved using only 2 sub-exposures with a mean S/N of 2560.

4.1.2 HIP 25848

HIP 25848 is a G0 weak-lined T Tau-type star (Li & Hu 1998). It has a trigonometric parallax of 7.95 ± 1.29 mas (van Leeuwen 2007) giving a distance of 410_{-57}^{+79} ly. Using the bolometric corrections by Bessell et al. (1998), the effective temperature was estimated to be 5700 ± 130 K. Using the formulation contained in Bessell et al. (1998) the star is estimated to be $\sim 1.67_{-0.17}^{+0.23} R_{\odot}$.

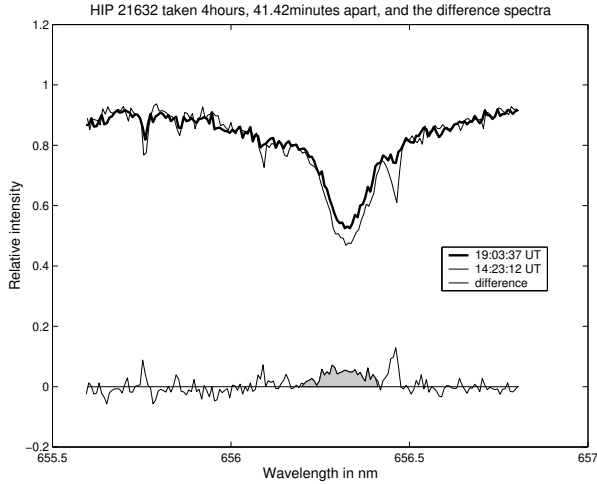


Figure 4: The variation of the $H\alpha$ profile of HIP 21632. Two exposures were taken, separated by 4 hours, 41.41 minutes. The variation in the $H\alpha$ profile is shown as a shaded region in the difference spectrum. The sharp absorption line at ~ 656.4 nm in the 12:23:12UT spectra is most likely due to telluric lines at 656.4049 and 656.4200 nm.

Placing this star on the theoretical isochrones of Siess, Dufour & Forestini (2000), it is estimated to be $1.3 \pm 0.1 M_{\odot}$ with an age between 10 Myr to 20 Myr. This is shown in Figure 5. This is consistent with the age found by Tetzlaff et al. (2011), however slightly less massive than that quoted in that paper. Norton et al. (2007) used SuperWASP to measure a period of 0.9426 d. This survey measured a $v \sin i$ of 69 km s^{-1} . This star has an emission equivalent width for the $H\alpha$ line of $668 \pm 60 \text{ mÅ}$, meaning that it is very active and one of the most active stars from this survey. The sodium doublet lines were filled in, almost to the continuum. It has a very deep LiI line suggesting, in the absence of a companion star, a youthful star. No spectropolarimetric observations were obtained were obtained. With a declination of $+23^{\circ}$, it would be a difficult target for ZDI at the AAT. However, this star would be an ideal target for ESPaDOnS at the CFHT (Canada-France-Hawaii Telescope, Hawaii) or NARVAL at the TBL (Télescope Bernard Lyot, Pic du Midi, France).

4.1.3 HIP 43720

HIP 43720 is a particularly active, G1V star (Torres et al. 2006). It has a trigonometric parallax of $5.38 \pm 0.94 \text{ mas}$ (van Leeuwen 2007) giving a distance of $606^{+128}_{-90} \text{ ly}$. Using the star's V-I value and the formulation in Bessell et al. (1998), the star's temperature was estimated to be $5700^{+40}_{-45} \text{ K}$ while its radius was estimated to be $2.6^{+0.7}_{-0.4} R_{\odot}$. Placing HIP 43720 onto the theoretical isochrones of Siess et al. (2000), as shown in Figure 5, suggests that this star's age is ≤ 10 Myr years and has a mass of between 1.6 and 1.8 M_{\odot} . However, this age estimate is not supported by the depth

of the LiI line, with an equivalent width of $< 5 \text{ mÅ}$. One can speculate that the lithium has already been depleted. Guillout et al (2009) suggest that stars with deep convective envelopes, such as M-dwarfs, are very efficient at depleting the lithium concentration. Being a pre-main-sequence star, HIP 43720 may also possess a very deep convective zone. Alternatively, Bouvier (2008) suggest that this depletion may be due to large velocity shear at the base of the convective zone as a result of star-disk interaction.

There is evidence of an active chromosphere with an emission equivalent width for the $H\alpha$ line of $\sim 400 \pm 28 \text{ mÅ}$ and strong emission in the magnesium triplet lines, as shown in Figure 1. Definite magnetic fields were observed on three occasions, however no magnetic field was detected on a fourth observation. On that occasion, the mean S/N was ~ 2626 . Figure 6 shows the Stokes V, null and Stokes I profile. This is an interesting target for follow-up spectropolarimetric studies at the AAT and as a result, is the subject of a forthcoming intense ZDI study (Waite et al., in preparation).

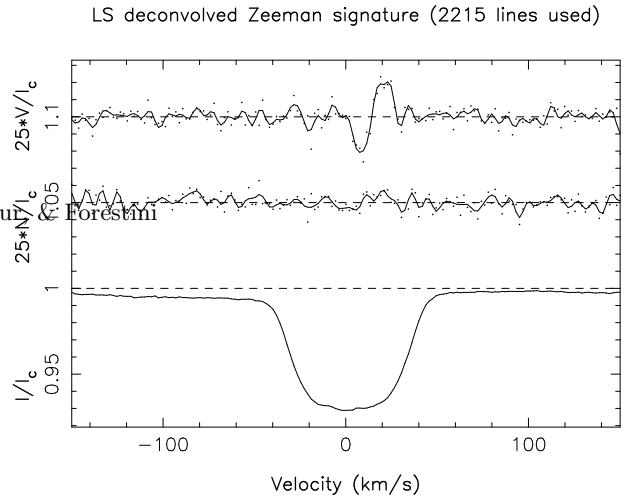


Figure 6: The various LSD profiles, as explained in Figure 3, for HIP 43720. The Stokes V profile (upper profile) shows evidence of a strong magnetic feature on the young star HIP 43720. The LSD profile (lower profile) has a flat bottom, possibly indicating the presence of a polar spot feature.

4.1.4 HIP 48770

HIP 48770 is a G7V pre-main-sequence star (Torres et al. 2006). It has a trigonometric parallax of $5.83 \pm 1.55 \text{ mas}$ (van Leeuwen 2007) giving a distance of $554^{+199}_{-115} \text{ ly}$. The $v \sin i$ was measured to be 35 km s^{-1} , which is consistent with that found by Torres et al. (2006). The radial velocity was determined to be 19.6 km s^{-1} , which is different from the 22.6 km s^{-1} observed by Torres et al. (2006). There appears to be no evidence of a secondary component in the spectra; but the presence of a companion in a large orbit cannot be ruled out. HIP 48770 is very young with a predominate

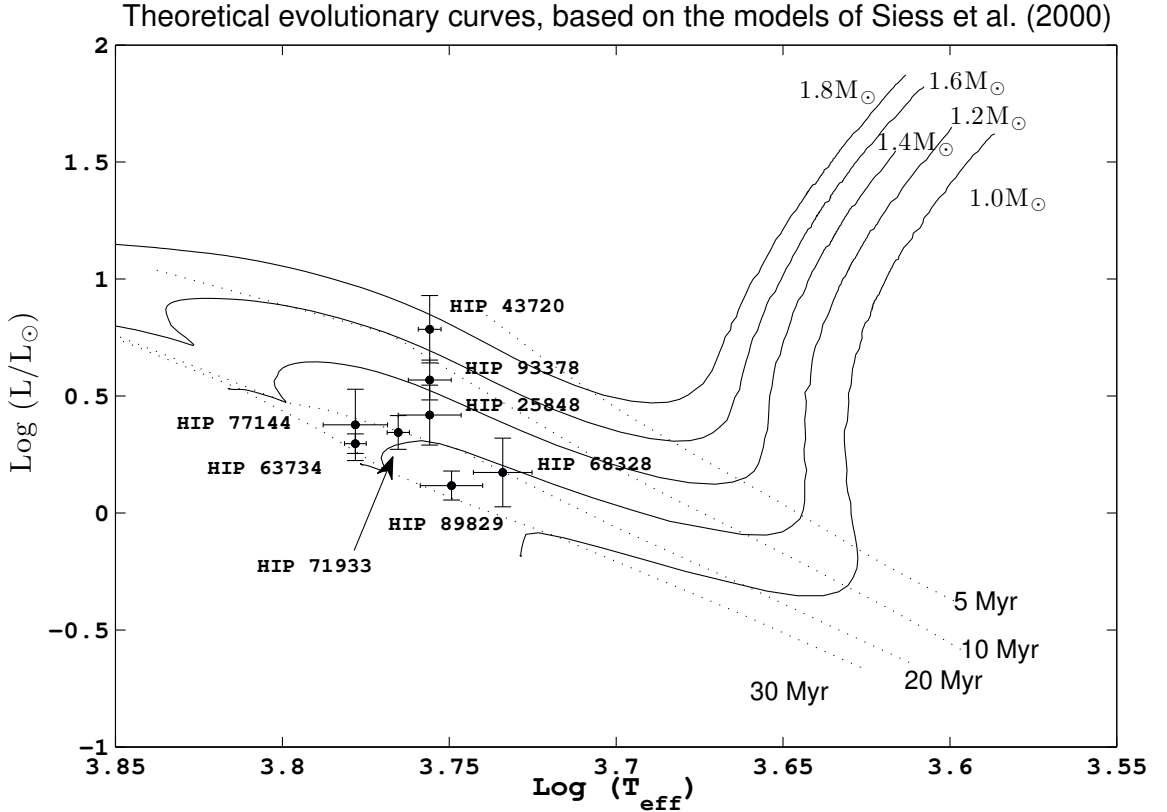


Figure 5: The evolutionary status of some of the survey stars, based on the theoretical isochrones of Siess et al. (2000). Only those likely ZDI targets with accurate photometry were incorporated onto this diagram.

lithium feature, as shown in Figure 2. Ammons et al. (2006) calculated an effective temperature of 5539 K. However, using the bolometric corrections of Bessell et al. (1998), our estimate is higher at 6000 ± 300 K. It is also very active with the $H\alpha$ spectral line being almost entirely filled in; and the magnesium triplet is also very strong. A visual magnitude of 10.5 would normally make it a challenging target for SEMPOL at the AAT. However, a magnetic detection was observed at the AAT demonstrating its highly active nature. The Stokes I LSD profile, along with the Stokes V profile is shown in Figure 7.

4.1.5 HIP 62517

HIP 62517 is an active G0 star (SAO Catalogue 1966). It has a parallax of 2.38 ± 1.6 mas (van Leeuwen 2007) giving a distance of 420^{+862}_{-169} ly. This star has a $v \sin i$ of 52 km s^{-1} . This particular star has a strong $H\alpha$ emission of 265 mÅ coupled with some filling in of the core of the magnesium triplet. However, its lithium line is rather weak, indicating that it may not be as young as some of the other stars in the sample. Ammons et al. (2006) calculated an effective temperature of 5336 K, which is slightly higher than our estimate of 5250 ± 65

K found using the bolometric corrections of Bessell et al. (1998). A marginal detection of a magnetic field was recorded on 2010, April 2, as shown in Figure 8. The S/N was 6685. Although only two snapshots were taken several months apart, with the indications that this star is single, the global magnetic field may be relatively weak and would be difficult to recover any magnetic features if observed over several epochs. This makes this star a difficult target for ZDI at the AAT.

4.1.6 HIP 71933

HIP 71933 is a pre-main-sequence F8V star (Torres et al. 2006). It has a parallax of 11.91 ± 0.99 mas (van Leeuwen 2007) giving a distance of 274^{+25}_{-21} ly. It has a projected rotational velocity of 75 km s^{-1} . The radial velocity was measured to be $\sim 4 \text{ km s}^{-1}$. As mentioned previously, the large spots on the surface of this star makes accurate radial velocity measurements difficult. However, Torres et al. (2006) measured 8.7 km s^{-1} while Gontcharov (2006) measured $12.3 \pm 0.4 \text{ km s}^{-1}$ and Kharchenko & Roeser (2009) measured $12.1 \pm 0.4 \text{ km s}^{-1}$. Perhaps this star is part of a wide binary system. Torres et al. (2006) flagged that this star might be a spectroscopic binary star. If the star was a bi-

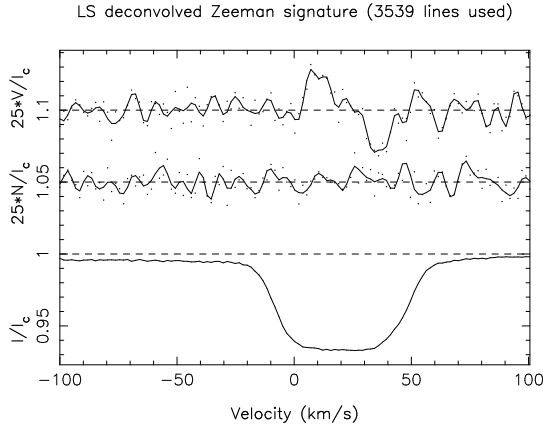


Figure 7: The various LSD profiles, as explained in Figure 3, for HIP 48770.

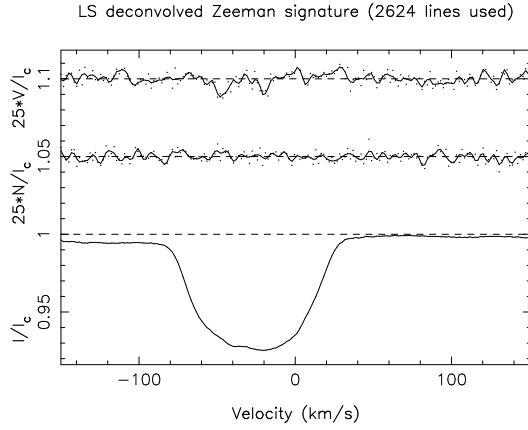


Figure 8: The marginal magnetic detection in the Stokes V profile (upper profile) for HIP 62517. The profiles are as explained in Figure 3.

nary, and the companion's profile is overlapping the primary's profile, it could be mistaken for spots. Alternatively, the companion may be a faint M-dwarf star thereby not deforming the profile at all. Careful consideration of the LSD profiles produced from the high-resolution spectra obtained using the normal UCLES setup ($R \sim 50000$) and spectropolarimetry ($R \sim 70000$), suggest that the deformations are due to spots rather than a companion. However, the presence of a secondary component cannot be ruled out by this survey.

Holmberg, Nordström, & Andersen (2006) estimated the effective temperature to be 5900K while Ammons et al. (2006) estimated the temperature to be 5938K. The equivalent width of the LiI was measured to be 139 ± 7 mÅ, after accounting for the FeI blended line using equation 1. When using the theoretical isochrones of Siess et al. (2000), as shown in Figure 5, this star's age is estimated to be ~ 20 Myr years and has a mass of $\sim 1.2 M_{\odot}$.

This is a particularly active star, as shown in Fig-

ure 1, with emission in the magnesium triplet lines and the H α line. However, there was some core emission in the NaI D₂, but not in the D₁ line. Spectropolarimetry was conducted on two occasions, once when the seeing was very poor (~ 2.5 to 3.5 arcsec) and only a S/N of 1748 but on the other occasion, reasonable seeing (~ 1.5 arcsec) resulted in a definite detection of a magnetic field. This detection is shown in Figure 9.

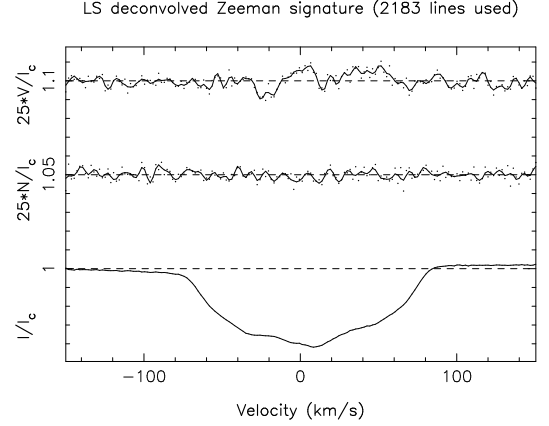


Figure 9: The various LSD profiles, as explained in Figure 3, for HIP 71933. The S/N for this was 8843.

4.1.7 HIP 77144

HIP 77144 is a post T-Tauri G1V star Sartori, Lépine, & Dias (2003) in the Scorpius-Centaurus group (Mamajek, Meyer, & Lieber 2002). It has a parallax of 7.12 ± 1.28 mas (van Leeuwen 2007) giving a distance of 458^{+100}_{-70} ly. It has a $v \sin i$ of 65 km s^{-1} with a particularly strong H α ($\text{EEW} = 466 \pm 24$ mÅ) and Li I lines ($\text{EqW} = 207 \pm 7$ mÅ). The temperature is estimated to be $\sim 6000 \pm 130$ K. It is approximately $1.45^{+0.25}_{-0.18} R_{\odot}$ when using the bolometric corrections of Bessell et al. (1998), giving a luminosity of $2.4^{+1.2}_{-0.7} L_{\odot}$. This young star, when placed on the theoretical isochrones of Siess et al. (2000) gives an age of this star of ~ 20 Myr and is approximately $1.3 \pm 0.1 M_{\odot}$. This is shown in Figure 5. The radial velocity was measured to be -1.6 km s^{-1} , which is consistent with that found by Madsen, Dravins, & Lindgren (2002) and Kharchenko et al. (2007) to within the respective errors of each measurement. A definite magnetic field was detected on 2010, March 31, with a mean S/N in the Stokes V profile of 4315. This magnetic detection is shown in Figure 10.

4.1.8 HIP 90899

HIP 90899 is a G1V star (Turon et al. 1993). According to Hipparcos database, this star has a parallax of 10.87 ± 1.34 mas (van Leeuwen 2007), giving a distance of 300^{+42}_{-33} ly. Using the V-I determined by the Hipparcos Star Mapper Photometry, a value of 0.62 ± 0.03 gives a temperature of 6090^{+130}_{-140} K using the formulation given in Bessell et al. (1998). This is consis-

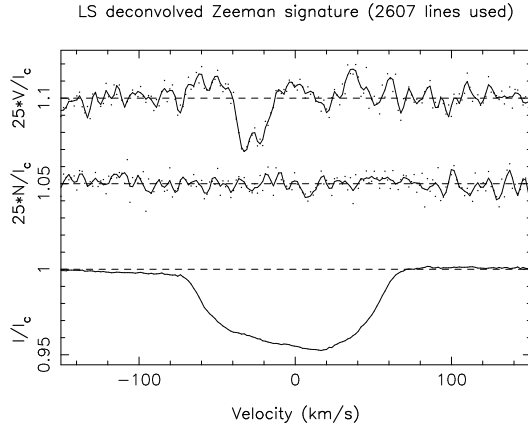


Figure 10: The various LSD profiles, as explained in Figure 3, for HIP 77144.

tent with other authors such as Wright et al. (2003) (6030 K) and Ammons et al. (2006) (5988 K). Using the bolometric corrections of Bessell et al. (1998) gives a radius of $0.97^{+0.1}_{-0.08} R_{\odot}$ and a luminosity of $1.13^{+0.37}_{-0.25} L_{\odot}$. This star has an emission equivalent width for the $H\alpha$ line of 408 ± 14 mÅ, with some filling of the core of the magnesium triplet lines, meaning that it is a very active star. It has a very deep LiI line with an equivalent width of 176 ± 6 mÅ, suggesting that, in the absence of a companion star, is youthful in nature. The magnetic detection, as shown in Figure 11 was only marginal but still, at a $v \sin i$ of 19 km s^{-1} , the magnetic topologies should be recoverable at the AAT.

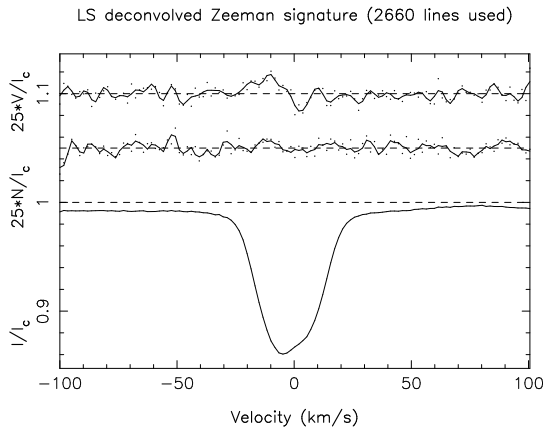


Figure 11: The various LSD profiles, as explained in Figure 3, for HIP 90899.

4.1.9 HIP 105388

HIP 105388 is a G7V pre-main-sequence star (Torres et al. 2006). This star has a $v \sin i$ of 17 km s^{-1} . This compares with the measurement of Torres et al. (2006) of

15.4 km s^{-1} . The value of this star's radial velocity was determined to be $-1.8 \pm 1.0 \text{ km s}^{-1}$. This value is consistent with those measured by Torres et al. (2006) of -0.9 km s^{-1} and Bobylev, Goncharov, & Bajkova (2006) $-1.6 \pm 0.2 \text{ km s}^{-1}$, to within the respective errors. This star has an emission equivalent width for the $H\alpha$ line of 520 mÅ, however, there is little core emission in either the magnesium triplet or sodium doublet. Zuckerman & Song (2004) proposed that HIP 105388 was a member of the Tucana/Horologium Association and an age estimate for this moving group, hence this star, is 30 Myr. Further indication of the youthful nature of this star is the very strong LiI line, as shown in Figure 1. Tetzlaff et al. (2011) estimate that this is a $1.0 \pm 0.1 M_{\odot}$ star. Whereas the $v \sin i$ is at the lower limit for ZDI at the AAT, a magnetic detection on this star was secured with an S/N of only 3822. There is limited spot activity as evidenced by the smooth Stokes I profile (lower LSD profile) in Figure 12. Recovering magnetic features from slow to moderate rotators is possible, as shown by Petit & Donati (2005) and Petit et al. (2008).

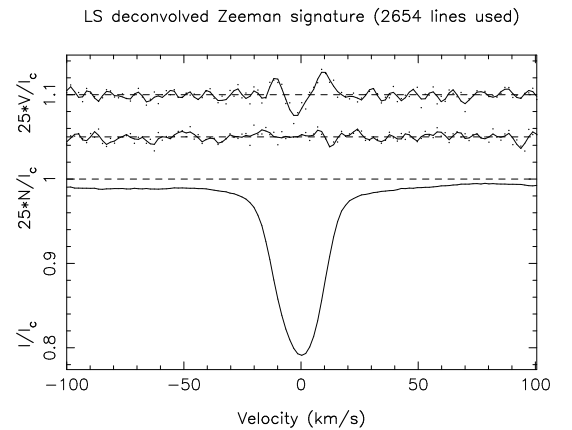


Figure 12: The various LSD profiles, as explained in Figure 3, for HIP 105388. The Stokes I LSD profile shows limited spot activity on the star yet there is a definite magnetic detection in the Stokes V profile. This is supported by the absence of signal in the null profile.

4.2 Ultra-Rapid Rotator: HIP 89829

HIP 89829 is a G5V star (Torres et al. 2006). With a $v \sin i$ of 114 km s^{-1} , this star has been classified as an URR. This measurement is consistent with Torres et al. (2006). Pojmański (2002) quote a rotational period of 0.570751d with a photometric amplitude of $\delta V = 0.07$. This star is very active and has an emission equivalent width for the $H\alpha$ line of 280 ± 52 mÅ yet little if any emission in the magnesium triplet or the sodium doublet is seen. It has a very deep, albeit broadened, lithium line with an equivalent width of 211 ± 13 mÅ. This indicates, in the absence of a companion star, a youthful star. This is consistent with that found by

Torres et al. (2006). When placed on the theoretical isochrones of Siess et al. (2000), this star is approximately 25-30 Myr and has a mass of between 1.0 and 1.2 M_{\odot} . The magnetic detection is shown in Figure 13. This is one of the most rapidly rotating stars that has had its magnetic field detected at the AAT.

As mentioned in Section 3.2, the large variation seen in the radial velocity measurements for HIP 89829 could be a result of this star being a binary star. However, after carefully considering the resulting LSD profiles from both the normal UCLES setup ($R \sim 50000$) and SEMPOL setup ($R \sim 70000$), we feel that this star is **probably** single.

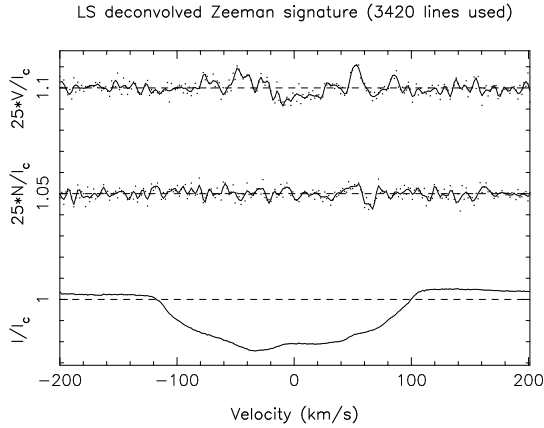


Figure 13: The various LSD profiles, as explained in Figure 3, for HIP 89829.

4.3 Hyper-Rapid Rotator: HIP 93378

HIP 93378 is a pre-main-sequence, G5V star (Torres et al. 2006). According to Hipparcos database, this star has a parallax of 9.14 ± 0.92 mas (van Leeuwen 2007), giving a distance of 357^{+40}_{-33} ly. It is a HRR with a $v \sin i$ of 226 km s^{-1} , which is consistent with the 230 km s^{-1} value measured by Torres et al. (2006) within the large uncertainty created by such a rapid rotation. This star's $H\alpha$ profile, when matched against a rotationally broadened solar profile, exhibited no emission in the core. Thus it appears that there is limited chromospheric activity occurring on this star. However, as mentioned previously, this lack of chromospheric emission may be due to the extreme broadening of the spectral lines thereby “washing out” the emission component. Another reason for this decreased $H\alpha$ emission may be due to supersaturation or even a modification of the chromospheric structure by the extremely strong shear forces as a result of such rapid rotation.

No magnetic detection was observed on this star, even when the data were binned to increase the relative signal-to-noise in excess of 9000. Again this extreme rotation may have simply washed out any magnetic signature. The resulting LSD profile is shown in Figure 14. Although this star is an extremely difficult target for ZDI at the AAT, its extreme rotation makes it an interesting target for Doppler imaging.

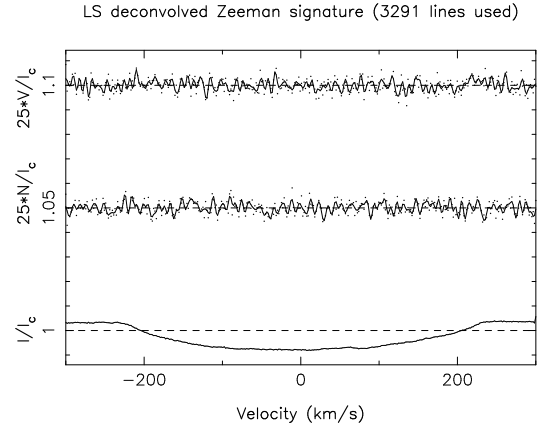


Figure 14: The various LSD profiles, as explained in Figure 3, for HIP 93378.

4.4 Active, young, slowly rotating stars.

This survey also found a number of slower rotating stars that are very young. Due to time constraints we did not take spectropolarimetric observations of these stars. However, the CFHT and TBL have been able to recover magnetic fields on slow rotators (Petit et al. 2008). One such star is the early G0 (Sartori, Lépine, & Dias 2003) star HIP 68328. It has a relatively slow rotation of $\sim 6 \text{ km s}^{-1}$. It has a parallax of 8.34 ± 1.56 mas (van Leeuwen 2007) giving a distance of 391^{+90}_{-61} ly. Using the bolometric corrections of Bessell et al. (1998), the temperature of HIP 68328 was estimated to be 5420^{+114}_{-107} K. This is consistent with the temperature estimated by Lafrasse et al. (2010) even though it is lower than the most recent estimate by Bailer-Jones (2011) of 5871 K. This project estimates that this star has a radius of $1.4^{+0.26}_{-0.17} R_{\odot}$, giving a luminosity of $1.49^{+0.78}_{-0.44} L_{\odot}$. This value is similar, within the relative error bars, to that estimated by Sartori, Lépine, & Dias (2003) of $1.66 L_{\odot}$. de Beeuw et al. (1999) identified this star as a possible member of the Scorpius-Centaurus OB association. This is a young star-forming region with stars less than 20 Myr old. When placing this star on the theoretical isochrones of Siess et al. (2000), as shown in Figure 5, the star has an age of $\sim 20 \pm 10$ Myr and a mass of $\sim 1.2 \pm 0.1 M_{\odot}$. This age is consistent with the observation of a very deep LiI line with an equivalent width of $263 \pm 4 \text{ mÅ}$. It has an emission equivalent width for the $H\alpha$ of $850 \pm 45 \text{ mÅ}$, the most active star in this sample by this measure. These observations of youth and activity are shown in Figure 15. Other slow rotators with substantial lithium lines include HIP 23316, HIP 41688, HIP 63734 and HIP 11241. All have indicators of having an active chromosphere with core emission in the $H\alpha$ line. Another interesting target is the slow rotator HIP 5617. It has very prominent emission in the wings of the $H\alpha$ line, extending above the continuum, indicating the presence of circumstellar material. However, the lithium line is very weak. This is perhaps a T-Tauri

star.

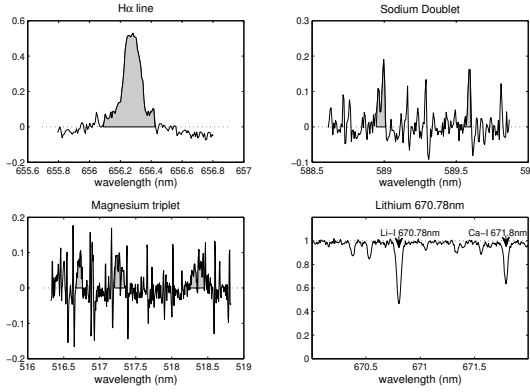


Figure 15: The activity indicators for HIP 68328. This star has a very strong emission component of the H α line with some moderate filling in of the sodium doublet and magnesium triplet. Also shown in this figure is the strong LiI 670.78 nm line.

4.5 Binary and Multiple Stellar Systems

The LSD profile is an excellent way of identifying a binary star (Waite et al. 2005), as the LSD profiles often show both stars, except if the star is undergoing an eclipse or is a faint star such as an M-dwarf. Where stars that appear to be rapidly rotating, more than one spectra (often two, three or more) were taken to make sure that the star was indeed single. HIP 31021, HIP 64732 and HIP 73780 were identified as binary stars based on their individual LSD profiles. HIP 64732 may have a giant polar spot on one of the components as one of the LSD profiles exhibited a “flat bottom”, indicating the likely presence of a giant polar spot or high latitude features. This is shown in top left panel of Figure 16. HIP 19072, HIP 67651 and HIP 75636 are likely to be spectroscopic binary stars while HIP 33111 could be a triple system. The associated LSD profiles are shown in Figure 16. There is a slight deformation of the LSD profile of HIP 75636 on the blue side that could be due to a companion star just moving into an eclipse of the second star. Also, the radial velocity of this star was measured to be $43.7 \pm 1 \text{ km s}^{-1}$ whereas Torres et al. (2006) measured the radial velocity to be 5.9 km s^{-1} . While some of the stars in this survey exhibit slight shifts in the radial velocity when compared with the work of Torres et al. (2006), this difference is far too great to conclude anything else except that it is a binary star.

Table 4 gives a summary of the likely targets for follow-up magnetic studies.

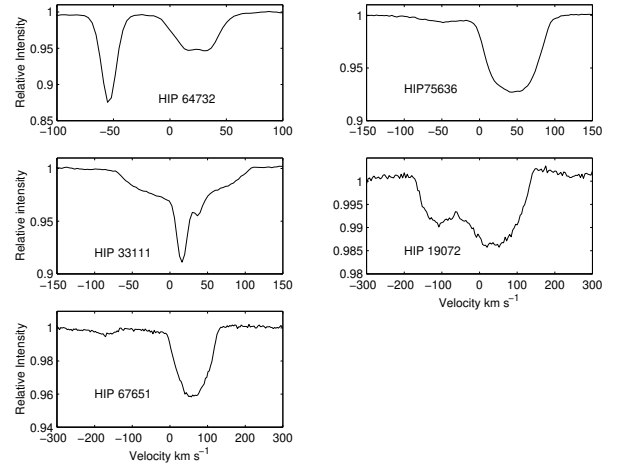


Figure 16: LSD profiles of some likely binary stars.

5 Conclusion

This survey aimed to determine the nature of a number of some unresolved variable stars from the Hipparcos database and to identify a number of targets for follow-up spectropolarimetric studies at the AAT. Of the 38 stars observed, three stars (HIP 31021, HIP 64732, HIP 73780) were spectroscopic binary stars while further three stars, (HIP 19072, HIP 67651 and HIP 75636) are likely to be a spectroscopic binary stars while HIP 33111 could be a triple system. Two stars rotate with speeds in excess of 100 km s^{-1} : HIP 93378 ($v \sin i \sim 226 \text{ km s}^{-1}$) and HIP 89829 ($v \sin i \sim 114 \text{ km s}^{-1}$). Magnetic fields were detected on a number of the survey stars: HIP 21632, HIP 43720, HIP 48770, HIP 62517, HIP 71933, HIP 77144, HIP 89829, HIP 90899 and HIP 105388. All of these stars would be suitable for follow-up spectropolarimetric studies using SEMPOL at the AAT.

Acknowledgments

The authors thanks the Director of the Australian Astronomical Observatory for allowing us some of his observing time to observe potential targets. This time will permit the expansion of our study into activity cycles on solar-type stars. We thank the referee of this paper, Pascal Petit, for his diligence and insightful comments that has made this a better paper. We thank J.-F. Donati on supplying ESPrIT. This project is supported by the Commonwealth of Australia under the International Science Linkages program. This project used the facilities of SIMBAD, HIPPARCOS and IRAF. This research has made use of NASA’s Astrophysics Data System.

References

Allende Prieto, C & Lambert, D.L., 1999, A&A, 352, 555

- Ammons, S.M., Robinson, S.E., Strader, J., Laughlin, G., Fischer, D., & Wolf, A., 2006, *ApJ*, 638, 1004
- Bailer-Jones, C.A.L., 2011, *MNRAS*, 411, 435
- Barnes S. A., Sofia S., Prosser C. F., Stauffer J. R., 1999, *ApJ*, 516, 263
- Bessell, M.S., Castelli, F., & Plez, B. 1998, *A&A*, 333, 231
- Bobylev, V.V., Goncharov, G.A., & Bajkova, A.T., 2006, *VizieR On-line Data Catalog: J/AZh/83/821* [Date accessed December 27, 2010]
- Bouvier, J., 2008, *A&A*, 489, 53L
- Brandenburg, A., Krause, F., Meinel, R., Moss, D. & Tuominen, I., 1989 *A&A*, 213, 411
- Brown, B.P., Browning, M.K., Brun, A.S., Miesch, M.S., & Toomre, J., 2010, *ApJ*, 711, 424
- Bruntt, H., De Cat, P., & Aerts, 2008, *A&A*, 478, 487
- Carter, B.D., Brown, S., Donati, J.-F., Rees, D., & Semel, M., 1996, *PASA*, 13, 150
- de Zeeuw, P.T., Hoogerwerf, R., de Bruijne, Brown, A.G.A., & Blaauw, A., 1999, *AJ*, 117, 354
- Dieckvoss W., & Heckmann O., 1975 *AGK3 Catalogue*, Hamburg-Bergedorf
- Donati, J.-F., Semel, M., & Rees, D.E., 1992, *A&A*, 265, 669
- Donati, J.-F., Semel, M., Carter, B.D., Rees, D.E., & Cameron, A.C., 1997, *MNRAS*, 291, 658
- Donati, J.-F., Collier Cameron, A., Semel, M., Hussain, G.A.J., Petit, P., Carter, B.D., Marsden, S.C., Mengel, M., López Ariste, A., Jeffers, S.V., & Rees, D.E., 2003, *MNRAS*, 345, 1145
- Donati, J.-F., & Landstreet, J.D., 2009, *ARA&A*, 47, 333
- do Nascimento Jr, J.D., da Costa, J.S., & De Medeiros, J.R., 2010, *A&A*, 529, 101
- Gontcharov, G.A., 2006, *AstL*, 32, 759
- Gray, D.F., 1992, *The Observation and Analysis of Stellar Photospheres*, 2nd edn (Cambridge: Cambridge University Press), 392
- Guillout, P., Klutsch, A., Frasca, A., Freire Ferrero, R., Marilli, E., Mignemi, G., Biazzo, K., Bouvier, J., Monier, R., Motch, G., Sterzik, M., 2009. *A&A*, 504, 829
- Holmberg, J., Nordström, B., & Andersen, J., 2009, *A&A*, 501, 941
- Houk, N., & Cowley, A.P., 1975, *Michigan catalogue for the HD stars*, vol. 1, Ann Arbor, Univ. of Michigan
- Houk, N., 1978, *Michigan catalogue for the HD stars*, vol. 2, Ann Arbor, Univ. of Michigan
- Houk, N., 1982, *Michigan catalogue for the HD stars*, vol. 3, Ann Arbor, Univ. of Michigan
- Houk, N., & Smith-Moore, M., 1988, *Michigan catalogue for the HD stars*, vol. 4, Ann Arbor, Univ. of Michigan
- Houk, N., & Swift, C., 1999, *Michigan catalogue for the HD stars*, vol. 5, Ann Arbor, Univ. of Michigan
- Irwin J., Hodgkin S., Aigrain S., Hebb L., Bouvier J., Clarke C., Moraux E., Bramich D. M., 2007, *MNRAS*, 377, 741
- Jackson J. & Stoy R.H., 1954, *Cape Photographic Catalogue for 1950.0 zone -30 to -64*, Ann. Cape Obs.
- Kharchenko, N.V., Scholz, R.-D., Piskunov, A.E., Röser, S., & Schilbach, E., 2007, *AN*, 328, 889
- Kharchenko, N.V., & Roeser, S., 2009, *VizieR On-line Data Catalog: I/280B/ascc* [Date accessed December 27, 2010]
- Koen, C., & Eyer, L., 2002, *MNRAS*, 331, 45
- Krishnamurthi A., Pinsonneault M. H., Barnes S., Sofia S., 1997, *ApJ*, 480, 303
- Kurucz, R.L., 1993, *CDROM #13 (ATLAS9 Atmospheric Models) and #18 (ATLAS9 and SYNTHE routines) spectral line databases*
- Lafrasse, S., Mella, G., Bonneau, D., Duvert, G., Delfosse, Z., & Chelli, A., 2010, *VizieR On-Line Data Catalog: II/300* [Date accessed February 19, 2011]
- Li, J.Z., Hu, J.Y., 1998, *A&AS*, 132, 173
- Madsen, S., Dravins, D., & Lindegren, L., 2002, *A&A*, 381, 446
- Mamajek, E.E., Meyer, M.R., & Liebert, J., 2002, *AJ*, 124, 1670
- Marino. A., Micela, G., Peres, G., & Sciortino, S., 2003, *A&A*, 407, L63
- Marsden, S.C., Carter, B.D., & Donati, J.-F., 2009, *MNRAS*, 399, 888
- Marsden, S.C., Jardine, M.M., Ramírez Vélez, E. Alecian, J.C., Brown, C.J., Carter, B.D., Donati, J.-F., Dunstone, N., Hart, R., Semel, M., & Waite, I.A., 2011a, *MNRAS*, 413, 1922
- Marsden, S.C., Jardine, M.M., Ramírez Vélez, E. Alecian, J.C., Brown, C.J., Carter, B.D., Donati, J.-F., Dunstone, N., Hart, R., Semel, M., & Waite, I.A., 2011b, *MNRAS*, 413, 1939
- Martín, E.L., & Claret, A., 1996, *A&A*, 306, 408
- Masana, E., Jordi, C., & Ribas, I., 2006, *A&A*, 450, 735

- Montes, D., Crespo-Chacón, I., Gálvez, M.C., Fernández-Figueroa, M.J., López-Santiago, J., de Castro, E.L., Cornide, J.m Hernán-Obispo, J., 2004, in “Lecture Notes and Essays in Astrophysics I” Proceedings of the Astrophysics Symposium held during the First Centennial of the Royal Spanish Physical Society, ed. A. Ulla and M. Manteiga, Madrid, 119
- Moss, D., Barker, D.M., Brandenburg, A. & Tuominen, I., 1995, *A&A*, 294, 155
- Norton A.J., Wheatley P.J., West R.G., Haswell C.A., Street R.A., Collier Cameron A., Christian D.J., Clarkson W.I., Enoch B., Gallaway M., Hellier C., Horne K., Irwin J., Kane S.R., Lister T.A., Nicholas J.P., Parley N., Pollacco D., Ryans R., Skillen I. & Wilson D.M., 2007, *A&A*, 467, 785
- Perryman, M.A.C., Lindegren, L., Kovalevsky, J., Høg, E., Bastian, U., Bernacca, P.L., Crézé, M., Donati, F., Grenon, M., Grewing, M., van Leeuwen, F., van der Marel, H., Mignard, F., Murray, C.A., Le Poole, R.S., Schrijver, H., Turon, C., Arenou, F., Froeschlé, M., & Petersen, C.S., 1997, *A&A*, 323, L49
- Petit, P., Donati, J.-F., & Collier Cameron, A., 2002, *MNRAS*, 334, 374
- Petit, P. & Donati, J.-F., 2005, Proceedings of the 13th Cambridge Workshop on Cool Stars, Stellar Systems and the Sun. ed. F. Favata, G.A.J. Hussain, and B. Battrick. ESA 560, 875
- Petit, P., Dintrans, B., Solanki, S.K., Donati, J.-F., Aurière, M., Lignières, F., Morin, F., Paletou, F., Ramirez, J., Catala, C. & Fares, R., 2008, *MNRAS*, 388, 80
- Pojmański, G., 2002, *Acta Astronomica*, 52, 397
- Prosser, C.F., Randich, S., Stauffer, J.R., Schmitt, J.H.M.M., & Simon, T., 1996, *AJ*, 112, 1570
- Randich, S., 1998, in *Cool Stars, Stellar Systems, and the Sun*, ASP Conf. Ser., ed. R. A. Donahue and J. A. Bookbinder, 154, 501
- Rousseau J.M., Perie J.P., & Gachard M.T., 1996, *A&AS*, 116, 301
- SAO Star Catalog J2000 [Date accessed December, 27, 2010]
- Sartori, M.J., Lépine, J.R.D., & Dias, W.S., 2003, *A&A*, 404, 913
- Semel, M., 1989, *A&A*, 225, 456
- Semel, M., Donati, J.-F., & Rees, D.E., 1993, *A&A*, 278, 231
- Siess, L., Dufour E., & Forestini, M. 2000 *A&A*, 358, 593
- Soderblom, D.R., Stauffer, J.R., Hudon, J.R., & Jones, B.F., 1993a, *ApJSS*, 85, 315
- Soderblom, D.R., Pilachowski, C.A., Fedele, S.B., & Jones, B.F., 1993b, *AJ*, 105, 2299
- Stauffer J. R., Hartmann L. W., Prosser C. F., Randich S., Balachandran S., Patten B. M., Simon T., Giampapa M., 1997, *ApJ*, 479, 776
- Tetzlaff, N., Neuhäuser, R., & Hohle, M.M., 2011, *MNRAS*, 410, 190
- Thatcher, J.D., & Robinson, R.D., 1993, *MNRAS*, 262, 1
- Torres, C.A.O., Quast, G.R., da Silva, L., de la Reza, R., Melo, C.H.F., & Sterzik, M., 2006, *A&A*, 460, 695
- Turon C., Egret D., Gomez A., Grenon M., Jahreiss H., Requieme Y., Argue A.N., Bec-Borsenberger A., Dommangeat J., Mennessier M.O., Arenou F., Chareton M., Crifo F., Mermilliod J.C., Morin D., Nicolet B., Nys O., Prevot L., Rousseau M., Perryman M.A.C 1993, *BICDS*, 43, 5
- van Leeuwen, F., 2007, *A&A*, 474, 653
- Vilhu, O., 1984, *A&A*, 133, 117
- Waite, I.A., Carter, B.D., Marsden, S.C., & Mengel, M.W., 2005, *PASA*, 22, 29
- Waite, I.A., Marsden, S.C., Carter, B.D., Hart, R., Donati, J.-F., Ramírez Vélez, J.C., Semel, M., & Dunstone, N., 2011, *MNRAS*, 413, 1949
- Wright, C.O., Egan, M.P., Kraemer, K.E., & Price, S.D., 2003, *AJ*, 125, 359
- Young, A., Skumanich, A., Stauffer, J.R., Bopp, B.W., Harlan, E., 1989, *ApJ*, 344, 427
- Zarro, D.M., & Rodgers, A.W., 1983, *ApJSS*, 53, 815
- Zuckerman, B., & Song, I., 2004, *ArA&A*, 42, 685

Table 2: Journal of Spectropolarimetric observations using SEMPOL at the AAT

HIP number	UTDATE	UT Time ^a	Exposure Time (seconds) ^b	Mean S/N ^c (Stokes <i>V</i>)	Magnetic Detection?	FAP ^d
21632	2008 Dec10	12:39:15	4 x 900	5898	No Detection	2.245×10^{-01}
21632	2008 Dec13	14:27:53	2 x 900 ^e	2710	Definite	4.761×10^{-06}
43720	2008 Dec09	16: 4:50	4 x 900	5304	Definite	0.000
43720	2008 Dec14	14:12:40	4 x 900	2626	No Detection	1.667×10^{-02}
43720	2009 Apr09	11: 8:13	4 x 800	3800	Definite	5.194×10^{-10}
43720	2009 Apr09	12:58:33	4 x 800	3759	Definite	6.871×10^{-12}
48770	2009 Dec03	16:42:47	4 x 750	1734	No Detection	1.528×10^{-02}
48770	2010 Apr01	10:30:40	4 x 800	2530	Definite	7.011×10^{-10}
62517	2009 Apr09	15: 7:23	4 x 800	1559	No Detection	8.504×10^{-01}
62517	2010 Apr02	12: 0:30	4 x 800	6685	Marginal Detection	1.786×10^{-03}
71933	2008 Dec18	17:44:15	4 x 900	1748	No Detection	7.146×10^{-01}
71933	2010 Apr01	15:37:08	4 x 800	8843	Definite	6.457×10^{-11}
77144	2010 Mar31	18:02:03	4 x 800	4315	Definite	0.000
77144	2010 Apr03	17:54:31	4 x 800	3783	No Detection	1.362×10^{-01}
89829	2009 Apr13	17:10:25	4 x 600	2544	No Detection	1.432×10^{-01}
89829	2010 Apr01	16:41:14	4 x 800	7274	Definite	4.663×10^{-15}
90899	2010 Mar28	17:50:20	2 x 800 ^e	669	No Detection	6.837×10^{-01}
90899	2010 Apr02	17:42:47	4 x 800	3663	Marginal Detection	3.647×10^{-3}
93378	2010 Apr01	17:43:42	4 x 800	9727	No Detection	7.102×10^{-2}
105388	2008 Dec09	10:17:50	4 x 900	3822	Definite	1.732×10^{-14}
105388	2008 Dec10	10:23:32	4 x 900	3388	No Detection	5.084×10^{-01}

^a Mid-observing time^b Generally a cycle consists of four sub-exposures.^c Mean Signal-to-noise in the Stokes *V* LSD profile, see Section 2.4.^d FAP: False Alarm Probability. See Section 3.5 for more details.^e Due to cloud, this cycle was reduced to two sub-exposures.

Table 4: New solar-type targets for Zeeman Doppler imaging.

Confirmed targets	HIP number
MR	21632, 90899, 105388
RR	43720, 48770, 62517, 71933, 77144
URR	89829
Potential targets ¹	
SR & MR	5617, 10699, 11241, 23316, 25848, 63734, 68328
HRR	93378 (DI target)
Binary Stars	
Binary Stars	31021, 64732, 73780
Probable Binary Stars	19072, 33111 ² , 67651, 75636

See Table 3 for definitions used in this table.

¹ Based solely on activity (if SR or MR) or rapid rotation.

² This star may even well be a triple system.